On the Decrease in Lateral Mobility of Phospholipids by Sugars

Geert van den Bogaart,* Nicolaas Hermans,* Victor Krasnikov,† Alex H. de Vries,‡ and Bert Poolman*
*Biochemistry Department, †Ultrafast Laser and Spectroscopy Laboratory, and ‡Molecular Dynamics Group, Groningen Biomolecular Science and Biotechnology Institute and Zernike Institute for Advanced Materials, University of Groningen, Nijenborgh 4, 9747 AG Groningen, The Netherlands

ABSTRACT Upon cold and drought stress, sucrose and trehalose protect membrane structures from fusion and leakage. Similarly, these sugars protect membrane proteins from inactivation during dehydration. We studied the interactions between sugars and phospholipid membranes in giant unilamellar vesicles with the fluorescent lipid analog 3,3′-dioctadecyloxacarbocyanine perchlorate incorporated. Using fluorescence correlation spectroscopy, it was found that sucrose decreased the lateral mobility of phospholipids in the fully rehydrated, liquid crystalline membrane more than other sugars did, including trehalose. To describe the nature of the difference in the interaction of phospholipids with sucrose and trehalose, atomistic molecular dynamics studies were performed. Simulations up to 100 ns showed that sucrose interacted with more phospholipid headgroups simultaneously than trehalose, resulting in a larger decrease of the lateral mobility. Using coarse-grained molecular dynamics, we show that this increase in interactions can lead to a relatively large decrease in lateral phospholipid mobility.

INTRODUCTION

Organisms from all kingdoms of life (1) accumulate disaccharides in response to various stresses, such as temperature (2), osmotic (3), and oxidative stress (4). Upon cold and drought stress, many organisms accumulate trehalose to protect both proteins and lipid membranes (see Oliver et al. (5) and Crowe et al. (6) for reviews). Higher plants often accumulate sucrose instead of trehalose (7). The protection of biological structures by sugars has applications in a wide range of fields, including food preservation and cryoconservation of eukaryotic cell lines (8). Recently, we showed that sucrose and trehalose (Fig. 1) protect membrane proteins from inactivation upon the conversion of large unilamellar vesicles (LUVs) to giant unilamellar vesicles (GUVs), which involves a cycle of dehydration and rehydration (9).

The ability of many sugars to protect lipid bilayers and proteins during freezing and drying has been established in several studies (5,6). Drying of membranes, composed of lipids with a low phase transition temperature (T_m), induces a transition from the liquid crystalline to the gel phase. This causes solute leakage, membrane fusion, and aggregation of membrane proteins. The protective effects of sugars are twofold: i), the formation of a glassy matrix, and ii), direct interactions between the lipids and the sugars (10–12). With a glassy matrix, the sugars form a hydration layer of amorphous glasses, preventing mechanical disruption and denaturation of (membrane) proteins. The formation of a glassy matrix is related to the glass transition temperature (T_g) of the sugars, and sugars with a high T_g generally provide better protection than sugars with a low T_g (7,10,11). Dehydration of membranes increases the T_m of the lipids and causes the liquid crystalline to gel phase transition, which has consequences for the membrane as permeability barrier and the conformational state of the embedded proteins. In the dry state, hydrogen-bond formation between the sugar molecules and the lipid headgroups reduces this increase of the T_m and thereby prevents the phase transition (6,10–12).

Of all tested sugars, trehalose ($T_g = 106$°C (13)) has been shown to cause the largest suppression of the T_m, offering the largest protection of vesicles and cells against solute leakage and fusion (5,6). However, disaccharides like sucrose ($T_g = 60$°C (13)) have been shown to also offer good protection against these membrane-rupturing events (14,15). In general, fructans provide better protection against solute leakage than glucans, whereas glucans provide better protection against membrane fusion (16). Both the suppression of the T_m and the formation of a glassy matrix are necessary for preventing membrane fusion, whereas the glassy matrix appears sufficient for the prevention of contents leakage from vesicles (11,16). Recently, it was found that the sugar/lipid ratios needed to prevent membrane fusion were 10-fold higher than those needed to suppress the T_m, and even higher ratios were needed to prevent solute leakage (12). Thus, despite a large number of studies on the protective effects of sugars on membranes, the precise interactions of these sugars with the lipids are poorly understood.

Most studies on the interactions between sugars and phospholipid membranes focus either on the T_m or on the protection against solute leakage and fusion of liposomes or whole cells, and little is known about the interactions between sugars and the lipids in the fully hydrated state. In solution, trehalose interacts directly with phospholipid bilayers, as was shown with Fourier transform infrared spectroscopy (17). These interactions must differ from the interactions in the dry state, because trehalose increased the T_m of fully hydrated lipid membranes in solution but not of membranes

Submitted August 31, 2006, and accepted for publication November 9, 2006.
Address reprint requests to Bert Poolman, Tel.: 31-50-363-4190; Fax: 31-50-363-4165; E-mail: b.poolman@rug.nl.

0006-3495/07/03/1598/08 $2.00
doi: 10.1529/biophysj.106.096461

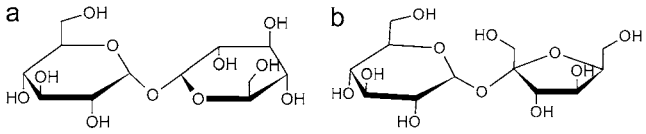

FIGURE 1 Trehalose (α-D-glucopyranosyl-α-D-glucropyranoside) (*a*) and sucrose (β-D-fructofuranosyl-α-D-glucopyranoside) (*b*).

in the dried state (18,19). Here, we report on sugar-membrane interactions, using fluorescence correlation spectroscopy (FCS) and molecular dynamics (MD) simulations. FCS was used to measure the influence of different sugars on the lateral diffusion of fully hydrated lipids in GUVs. The MD simulations were used to rationalize the observed differences in diffusion coefficients.

METHODS

GUV formation

For the formation of GUVs, 1 μl of a solution of 10 mg ml^{-1} lipids was dried in vacuum at room temperature on an ultraviolet-ozone cleaned cover glass and rehydrated for 2 h in 10 mM potassium phosphate, pH 7.0, with the sugar present. The lipid mixtures were composed of either pure DOPC (1,2-dioleoyl-*sn*-glycero-3-phosphatidylcholine) or a mixture of DOPC and DOPS (1,2-dioleyl-*sn*-glycero-3-phosphatidylserine, Avanti Polar-Lipids, Alabaster, AL) at a 3:1 molar ratio. For FCS, the fluorescent lipid analog 3,3′-dioctadecyloxacarbocyanine perchlorate (DiO; Invitrogen, Carlsbad, CA; excitation and emission wavelengths of 484 and 499 nm, respectively) was incorporated at a DiO/lipid ratio of 1:10,000 molar.

Fluorescence correlation spectroscopy

FCS measurements were carried out on a laser scanning confocal microscope (9), based on an inverted microscope Axiovert S 100 TV (Zeiss, Jena, Germany) in combination with a galvanometer optical scanner (model 6860, Cambridge Technology, Watertown, MA) and a microscope objective nanofocusing device (P-721, Physik Instrumente, Karlsruhe/Palmbach, Germany). For excitation of the fluorescent lipid analog DiO, an argon ion laser (488 nm, Spectra-Physics, Mountain View, CA) was focused by a Zeiss C-Apochromat infinity-corrected 1.2 numerical aperture 63× water immersion objective. The intensity of the laser beam did not exceed 10 μW at the back aperture of the objective. Emission was collected through the same objective, separated from the excitation beam by a beam pick-off plate (BSP20-A1, ThorLabs, Newton, NJ) and directed through an emission filter (HQ 535/50, Chroma Technology, Rockingham, VT) and a pinhole (diameter of 30 μm) onto an avalanche photodiode (SPCM-AQR-14, EG&G, Albuquerque, NM). The fluorescence signal was digitized, and the autocorrelation curve was calculated using a multiple τ algorithm. The setup was calibrated by measuring the known diffusion coefficient of Alexa fluor 488 in water (Invitrogen; $D = 300$ μm^2 s^{-1}). The lateral radius ω_{xy}, defined as the point where the fluorescence count rate per molecule decreased e^2 times, was 180 nm, corresponding to a detection volume of ~0.20 fl.

For the FCS measurements, the focal volume was positioned at the upper pole of a GUV, as described in Doeven et al. (9). For each sample, the fluorescence autocorrelation of 10 GUVs was measured for 80 s. The fluorescence autocorrelation curves were fitted with a model for two-dimensional Brownian motion (20). The viscosities of the sugar solutions were determined by measuring the diffusion constant of free Alexa fluor 488 in the various solutions. The diffusion constant is linearly related to the viscosity, as described by the Einstein-Stokes model.

General atomistic MD simulation conditions

All MD simulations at atomistic scale were performed using the GROMACS code (21), with parameters based on the GROMOS force field parameter set 53A6 (22). The simple point charge water model (23) was used to model water. Newton's equations of motion were integrated using the leapfrog algorithm (24) with a 2-fs time step. The LINCS method (25) was applied to constrain all bond lengths. The water geometry was constrained using the SETTLE algorithm (26). The simulations were carried out in a rectangular box with an isothermal-isobaric (NPT) ensemble at 300 K, using a Berendsen thermostat (27), with a coupling constant of 0.1 ps. The pressure was coupled semiisotropically using a Berendsen scheme (27) with a reference pressure of 1 bar in all directions, a relaxation time of 1 ps, and an isothermal compressibility of 5×10^{-5} bar^{-1}.

The nonbonded interactions were calculated using a twin-range cutoff scheme. All Lennard-Jones and electrostatic interactions within the 0.9-nm short-range cutoff were evaluated every time-step, based on a pair list recalculated every 10 steps. The Lennard-Jones potentials and electrostatic interactions within the long-range cutoff distance of 1.4 nm were calculated simultaneously with each pair list update and assumed constant in between. Electrostatic interactions beyond the 1.4-nm cutoff radius were corrected with a reaction field potential, with $\varepsilon_r = 62$ (28). For analysis, the atomic coordinates were saved every 50 ps. The MD data were analyzed using the standard GROMACS tools (21) as described in De Vries et al. (29) and Pereira et al. (30).

Used topologies

The topologies of both sucrose (β-D-fructofuranosyl-α-D-glucopyranoside) and trehalose (α-D-glucopyranosyl-α-D-glucropyranoside) for the atomistic MD simulations were generated from protein data bank files (31), using the Dundee PRODRG2 server (32). The force field parameters to describe trehalose were modified according to Lins and Hünenberger (33). The force field parameters to describe sucrose were derived starting from the force field parameters of hexopyranose-based carbohydrates (33) with respect to bond angle bending, bond stretching, dihedral deformation, improper dihedral deformation, and van der Waals interactions. For the partial charges, the classical electrostatic potential outside the sucrose molecule was fitted to the corresponding quantum-mechanical potential. Redistribution of charges was required to permit the definition of neutral charge groups with restricted sizes within the molecule, similar to that in Lins and Hünenberger (33). During the 10-ns simulations, both sugars stayed in solution up to 1.5 M, as expected from the solubility of the sugars. The topology files are provided in the Supplementary Material.

Description of initial conditions and systems

The starting conditions for the atomistic MD simulations of trehalose and sucrose with DOPC bilayer were created by deleting the water molecules from a system with an equilibrated DOPC bilayer (29). The DOPC bilayer consisted of two monolayers of 32 lipids each. A total of 16, 32, or 60 trehalose or sucrose molecules were added to this system, and the box was filled with water molecules, resulting in sugar concentrations of 0.4, 0.8, and 1.5 M, respectively. The final lipid/water ratio was higher than 1:25 molal, so the lipid bilayer was fully hydrated. The systems were equilibrated for 10 ns at 300 K, after which most of the sugars were adsorbed on the bilayer interface with the lipid headgroups, and these systems were taken as starting conditions for further simulations.

Coarse-grained MD simulations

All coarse-grained MD simulations were performed using the GROMACS code (21). Newton's equations of motion were integrated using the leapfrog algorithm (24) with a 5-fs time step. The bonds and angles were represented by a harmonic potential. The simulations were carried out in a rectangular

box of fixed size (25 × 25 × 10 nm) with the temperature at 325 K, using a Berendsen thermostat (27), with a coupling constant of 0.1 ps. The Lennard-Jones potentials and forces were calculated using the shift potential implemented in GROMACS (21), which decreases potentials and forces smoothly to zero at the cutoff of 1.2 nm (34). A twin-range cutoff scheme was used with a short-range cutoff of 0.9 nm, and a long-range cutoff of 1.2 nm, with a neighbor list that was updated every 10 time steps. For analysis, the atomic coordinates were saved every 50 ps.

The lipids were represented by rods consisting of two beads and the sugars as squares consisting of four beads, with masses of 72 amu per bead. The length of all bonds between the beads was 0.47 nm with a 1250 kJ mol^{-1} nm^{-2} harmonic force constant. The interactions between molecules were either attractive or semiattractive, where the Lennard-Jones parameters were $4\,\varepsilon_i\sigma_i^6 = 0.216$ kJ mol^{-1} nm^6 and $4\,\varepsilon_i\sigma_i^{12} = 0.232 \times 10^{-2}$ kJ mol^{-1} nm^{12} for the attractive interactions and $4\,\varepsilon_i\sigma_i^6 = 0.181$ kJ mol^{-1} nm^6 and $4\,\varepsilon_i\sigma_i^{12} = 0.195 \times 10^{-2}$ kJ mol^{-1} nm^{12} for the semiattractive interactions. The interactions between lipid molecules and between sugar molecules were set to semiattractive. The interaction between each of the beads of the sugar molecules with the lipid molecules was varied from attractive to semiattractive. All interaction sites were uncharged. The lipids and the sugars were kept in two planes using positional restraints in the direction perpendicular to the planes with force constants 1000 kJ mol^{-1} nm^{-2} and 100 kJ mol^{-1} nm^{-2}, respectively. The planes of the lipids and of the sugars were 0.5 nm apart. A total of 1024 lipid molecules and 512 sugar molecules was simulated for 500 ns.

RESULTS

Fluorescence correlation spectroscopy

In the absence of sugar, and using FCS on GUVs, a lateral diffusion constant D of the fluorescent lipid analog DiO was measured at 6.5 ± 0.6 μm^{2}s^{-1}. This value is in agreement with values determined by means of FCS (9,35) and pulsed field gradient NMR (36). Addition of sugars up to 2 M reduced the lateral mobility in a concentration-dependent manner; the maximal decrease in D was ~2.5-fold and observed for sucrose. For all concentrations, sucrose inhibited the diffusion of lipids more than maltose and trehalose (Fig. 2 *a*). This larger inhibition of the phospholipid diffusion by sucrose was observed both in membranes consisting of a 3:1 molar ratio of DOPC/DOPS and in membranes consisting of pure DOPC (not shown). The decrease by sugars could not be fully attributed to an increase in the viscosity of the bulk phase as predicted by Saffman and Delbrück (Fig. 2 *b*) (37).

The two monosaccharides fructose and glucose, of which sucrose is composed, decreased the lateral mobility to a lesser extent than sucrose (Fig. 2 *c*). In addition, a range of other (oligo)saccharides was tested: glucose, maltose, maltotriose, and maltotetrose (only estimated up to 0.8 M because of limited solvability), with increasing hydrogen-bonding capabilities. Although there appeared to be a trend that longer saccharides caused a stronger decrease in the lateral mobility of lipids, the decrease was not as large as that by sucrose (Fig. 2 *d*), indicating that the effect was not related to an increased viscosity of the bulk phase. Sucrose thus inhibited the lateral diffusion more than all the other sugars tested, suggesting a stronger interaction of sucrose with the lipids.

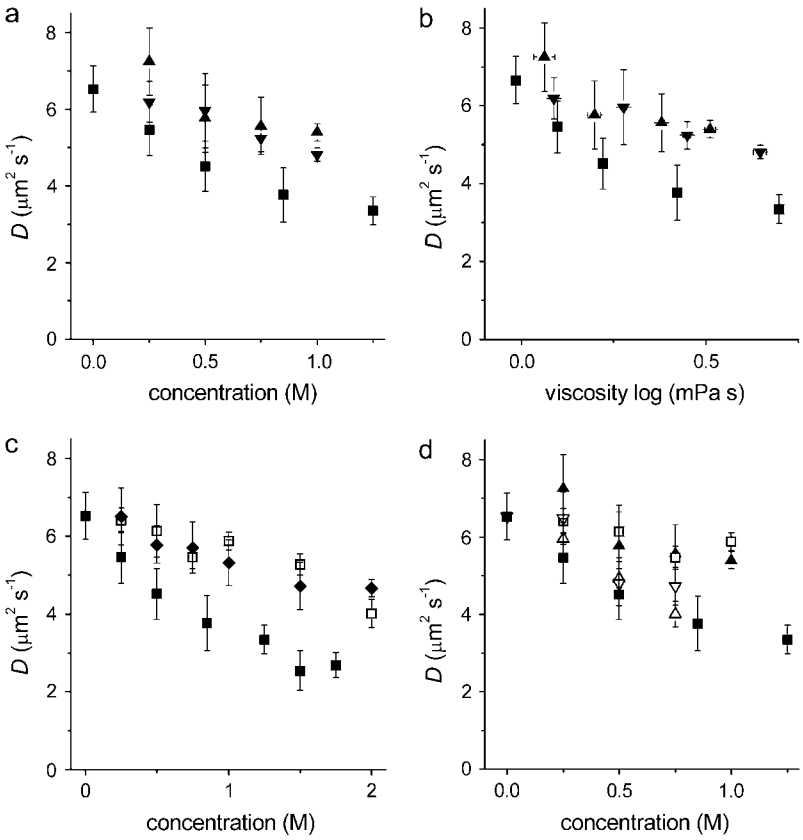

FIGURE 2 Sugars decrease the lipid mobility. The diffusion of the fluorescent lipid analog DiO in membranes consisting of a 3:1 molar mixture of DOPC/DOPS is shown. On the x axis, the bulk concentrations (*a*) and viscosities (*b*) of sucrose (■), trehalose (▼), and maltose (▲), and the bulk concentrations of (*c*) sucrose (■), glucose (□), and fructose (♦), and (*d*) sucrose (■), glucose (□), maltose (▲), maltotriose (∇), and maltotetrose (Δ) are plotted.

MD simulations

MD simulations at an atomistic scale were performed in an attempt to rationalize the differences in the interactions between sucrose and trehalose with the lipid membrane. Seven simulations were performed: a DOPC bilayer in water without sugar and DOPC bilayers in water with 0.4, 0.8, and 1.5 M sucrose or trehalose, all at 300 K. After 10-ns equilibration time, all simulations were performed for 100 ns. During the 10-ns equilibration time, a steady state was reached (not shown), in accordance with published data (30,38,39). The projected area per lipid during the simulations was independent of the sugar concentrations and was 58.4 ± 0.8 Å^2. This value is lower than experimental values for pure DOPC of 59.4 (40) to 72.2 ± 0.5 Å^2 (41,42). The area per lipid is known to be lower in comparison to experimental ones when using the GROMOS 53A6 force field (22,43). Since the lipids were still in the liquid crystalline phase, the simulations were used to provide qualitative information regarding the interactions between the lipid headgroups and the sugars.

Fig. 3 shows a snapshot of the 0.8-M sucrose system after 100 ns of simulation time. It shows that most of the sucrose molecules interact with the lipid headgroups, leading to an increase in the surface concentration. The density profiles perpendicular to the membrane of different atom groups for the 0.8-M sucrose and trehalose systems are presented in Fig. 4. The density profiles show that both sucrose and trehalose were adsorbed at the DOPC bilayer interface. No differences in protrusion were observed between sucrose and trehalose or between the glucose and fructose moieties of sucrose.

In addition to the starting condition where the sugars were added to an existing DOPC bilayer, a random mixture of sugar, water, and DOPC molecules was simulated. Within 10 ns of simulation time, a bilayer formed spontaneously (44), with the sugars interacting in a similar way as in the simulations where a DOPC bilayer was present from the start. This indicates that the interaction is not an artifact of the starting conditions or the timescale of the simulation.

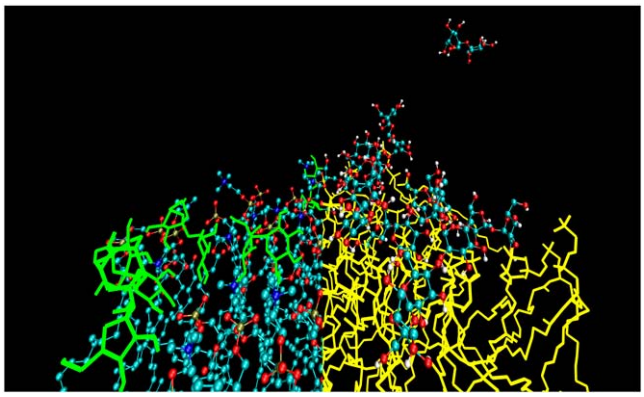

FIGURE 3 The MD simulations. Snapshot taken from an MD simulation of a DOPC bilayer with 0.8-M sucrose system after 100 ns. Only one of the leaflets of the bilayer is shown. For clarity, the sucrose molecules are presented in green on the left side of the figure, whereas the lipids are presented as ball and stick, with the carbon atoms shown in blue, the oxygen atoms shown in red, and the hydrogens in white. Only hydrogens capable of forming hydrogen bonds are shown. On the right side of the figure, the lipids are presented in yellow and the sucrose in ball and stick representation.

In the absence of sugar, a lateral diffusion constant for the lipids of $D = 4.7 \pm 3.2$ μm^{2}s^{-1} was obtained, which is in good agreement with the measured value of $D = 6.5 \pm 0.6$ μm^{2}s^{-1}. The distribution of the diffusion constants of the individual lipids was wide, as can be seen in the histogram in Fig. 5, and is also reported in De Vries et al. (29). If the simulation time is increased, the diffusion constants should converge to the same value. However, MD simulations of DPPC bilayers showed only a small narrowing of the spread of the diffusion constants between 100- and 500-ns simulation (data not shown). Because of this broad distribution, it was not possible to calculate D reliably from the trajectories, and the data had to be interpreted qualitatively. It is clear that both sucrose and trehalose reduced the lateral mobility of the lipids at all three concentrations (Fig. 5). Due to the qualitative nature of the results, however, no statistically significant difference between sucrose and trehalose could be observed in the simulations.

Next, the interactions of sucrose and trehalose with the lipid layer were analyzed in terms of hydrogen bonding (Fig. 6). The analysis should be considered as an indication for hydrogen-bond formation. A hydrogen bond was considered present if an acceptor and a donor atom were within a distance of 0.35 nm of each other, and donor-hydrogen-acceptor formed an angle smaller than 30°. For all sugar concentrations, sucrose formed ~10% more hydrogen bonds per sugar with lipid headgroups than trehalose (Fig. 6 *a*). The lifetime of the hydrogen bonds did not significantly differ between sucrose and trehalose. The average number of mutual hydrogen bonds between the sugar molecules was not different for sucrose and trehalose (Fig. 6 *a*). Most hydrogen bonds between sugars and lipid headgroups were formed with the phosphate oxygens. The average number of sugar molecules that formed hydrogen bonds with a lipid was significantly larger for sucrose than for trehalose (Fig. 6 *b*), and the average number of lipids that formed hydrogen bonds with a sugar was also larger (Fig. 6 *c*). For the 0.8-M sugar concentrations, the distribution of the number of lipid molecules bound per sugar is shown in Fig. 6 *d*. In summary, sucrose interacted with more lipid molecules at the same time as trehalose.

To assess whether an increased number of interactions between the sugar molecules with the phospholipids can result in a decrease of the lateral mobility of the phospholipids, coarse-grained simulations were performed. The lipids were represented as rods consisting of two beads and the sugars as rectangles consisting of four beads (Fig. 7 *a*). The lipids were confined to move in a plane, as were the sugars. The respective planes were 0.5 nm apart, but some

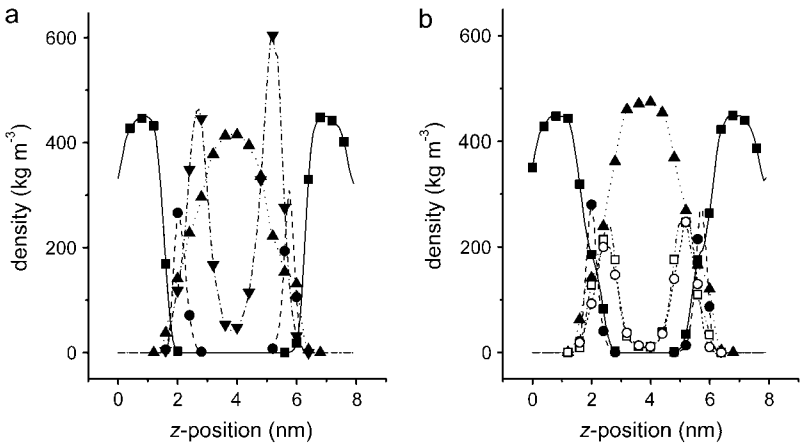

FIGURE 4 Density profiles along the axis perpendicular to the membrane for the 0.8-M sugar simulations. (*a*) The mass densities are shown of trehalose (▼), water (▲), and the headgroups (●) and tails (■) of DOPC. (*b*) The same as for (*a*), only with the densities for the glucose (○) and fructose (□) moieties of sucrose plotted separately. For clarity of the figure, symbols spaced 0.4 nm apart are plotted.

movement of the molecules perpendicular to the planes was allowed. The affinity of the lipid beads to each of the sugar beads was varied from semiattractive to attractive, modeling different levels of interaction between the sugars and the lipids and reflecting the hydrogen-bonding capacity. The lateral diffusion of the lipids decreased when the number of sugar beads that had attractive interactions to the lipid beads increased from 0 to 3 (Fig. 7 *b*).

DISCUSSION

Fluorescence correlation spectroscopy

In this study, we assessed the interaction between sugars and lipid bilayers using FCS. We show that sugars reduced the lateral mobility of phospholipids in the fully hydrated, liquid crystalline membrane. Interestingly, for all sugar concentrations, sucrose slowed down the lipid diffusion more than the other sugars, including trehalose. Since trehalose and sucrose solutions have a similar viscosity, the often used Saffman-Delbrück model (37), which describes the relationship between lateral diffusion and the viscosity of the bulk phase, fails. Furthermore, one of the main assumptions of the model is that the membrane forms a homogeneous two-dimensional medium and that the radius of the molecules the membrane consists of are infinitely smaller than the radius of the diffusing particles. In the case of lipids, this assumption is obviously not satisfied, and the Saffman-Delbrück model has inherent limitations (45).

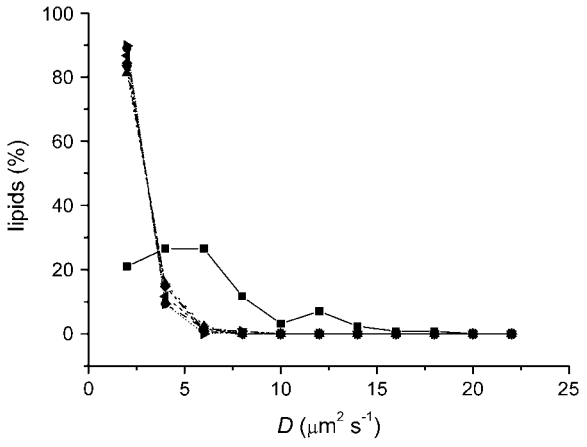

FIGURE 5 Distribution of the diffusion constants of the lipids obtained from the MD simulations with no sugar (■), 0.4 M (●), 0.8 M (▲), or 1.5 M (▼) sucrose, and 0.4 M (♦), 0.8 M (◄), or 1.5 M (►) trehalose.

The decrease of the lateral phospholipid mobility by sucrose was also larger than that of the trisaccharide maltotriose and the tetrasaccharide maltotetrose, which have more hydrogen-bonding capabilities. Maltotriose is known to protect membranes against leakage upon freezing and drying (19,46). The stronger decrease in the lateral mobility by sucrose than that by other sugars is unlikely to be an artifact due to the use of the fluorescent lipid analog DiO, since the analog NBD C_6-HPC showed a similar effect (9). NBD C_6-HPC has a fluorescent moiety in the lipid tail rather than the headgroup like DiO. Furthermore, the measured effect was present in membranes consisting of pure DOPC and of a mixture of DOPC and DOPS.

The large decrease of the lateral mobility by sucrose has not been reported previously. Two experimental studies regarding the effect of sugars on the diffusion of lipids have been published (47,48), both using the alcohol sugar glycerol. A fluorescence recovery after photobleaching (FRAP) study showed that the diffusion constant decreased linearly with the sugar concentration (47), whereas an excimer formation study showed a much smaller effect, ~2-fold (48). For glycerol, we measured an inhibition of the lateral phospholipid mobility of ~1.5-fold (not shown), which is in agreement with the excimer formation study (48). In the FRAP study (47), a fluorescent-labeled transmembrane lipid was used in multilayer lipid sheets, and this configuration might have influenced the diffusion of the lipid probe. Neither of these studies explored sucrose or trehalose.

MD simulations

MD simulations by Pereira et al. (30) and recently Skibinsky et al. (38) showed interactions between trehalose and lipid

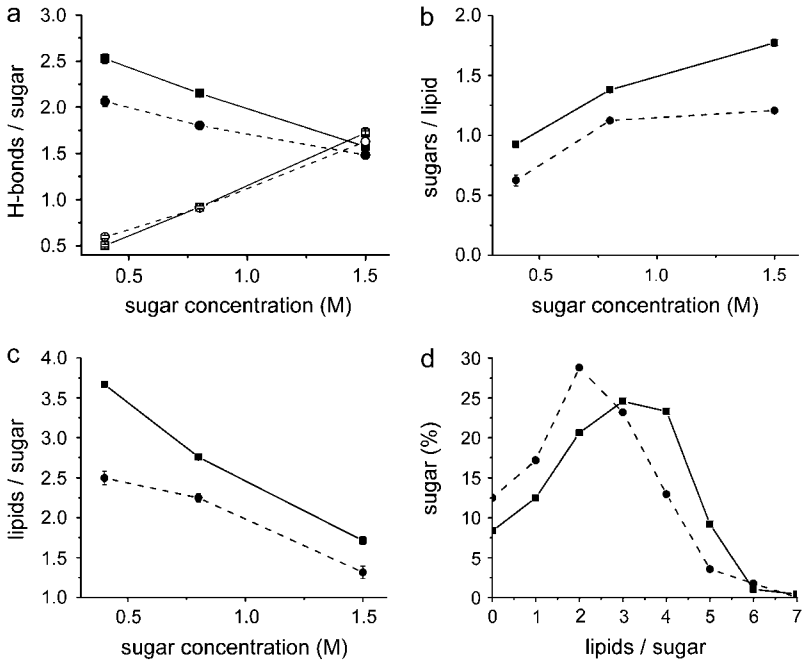

FIGURE 6 Hydrogen-bond analysis. (*a*) The average number of hydrogen bonds between the sugar molecules and the lipids (*solid symbols*) or between sugar molecules (*open symbols*) for sucrose (■, □) and trehalose (●, ○). (*b*) The average number of sucrose (■) and trehalose (●) molecules that formed hydrogen bonds with a lipid. (*c*) The average number of lipids that formed hydrogen bonds with a sucrose (■) or trehalose (●) molecule. (*d*) Distribution of the number of lipids that bound to a sucrose (■) or trehalose (●) molecule (for 0.8 M of sugar).

headgroups similar to our observations, but sucrose was not investigated. An MD study, where both sucrose and trehalose were included, was performed by Sum et al. (39). They showed that both trehalose and sucrose inserted into the bilayer and interacted with multiple lipid molecules simultaneously, which is in agreement with our simulation. However, due to the length of these simulations (~10 ns), no significant diffusion constant of the phospholipids could be calculated. Furthermore, the hydrogen bonds were not analyzed to the same extent as in our work. Therefore, at the start of this project, no model was available to explain the effect of different sugars on the lateral lipid mobility. We ran longer (100-ns) simulations to be able to model the influence of the sugars on the lipid headgroups. The lipid bilayers were fully hydrated so we could compare our FCS measurements with the MD simulations.

Our MD simulations at atomistic scale show that both sucrose and trehalose slow down the lateral diffusion of the lipids, although no difference between the sucrose and the trehalose was observed due to the limited timescale of the simulations. A more extensive analysis of the MD data showed that sucrose formed ~10% more hydrogen bonds with phospholipid headgroups than trehalose (Fig. 6), whereas the lifetimes of the hydrogen bonds were similar. Furthermore, sucrose interacted with more lipid headgroups simultaneously than trehalose. Coarse-grained model simulations showed that an increased cross-linking of lipids by sugars can result in a relatively large reduction of the diffusion constant (Fig. 7). Based upon these observations, it is concluded that sucrose is more efficient in cross-linking the lipid headgroups than trehalose. The result is a stronger reduction of the lateral lipid mobility and provides an explanation for the FCS data.

In summary, using FCS we showed that sucrose decreases the lateral mobility of lipids more than trehalose. Atomistic and coarse-grain MD simulations provide an explanation for the differences these sugars exert on the lateral mobility of lipids. Relatively small differences in the interactions

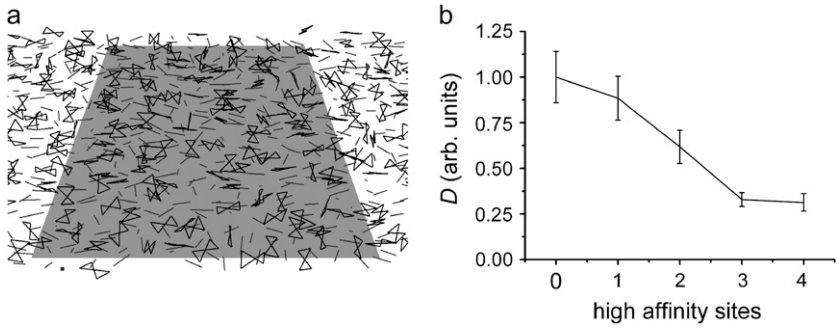

FIGURE 7 Increased cross-linking decreases the lipid mobility. (*a*) Snapshot of a coarse-grained MD simulation. The lipids are represented by small rods consisting of two beads (*dark gray*), whereas the sugars are represented by rectangles consisting of four beads (*black*). The position of the molecules is restrained to planes parallel to the light gray square. The affinity of each of the sugar beads to the lipids can be varied. A total of 1000 lipids and 500 sugar molecules were simulated in the unit cell, but only a fraction is shown. (*b*) Diffusion constant obtained from the coarse-grained simulation as a function of the number of high affinity beads of the sugar, relative to the lipid with weakly interacting sugar.

between sugars and phospholipids result in relatively large effects on the lipid mobility. These different interactions may also lead to differences in membrane protection.

SUPPLEMENTARY MATERIAL

An online supplement to this article can be found by visiting BJ Online at http://www.biophysj.org.

We are grateful to the Netherlands Science Foundation (NWO), Earth and Life Sciences (ALW; grant number 814.02.002), and the Zernike Institute for Advanced Materials for financial support.

REFERENCES

1. Crowe, J. H., J. F. Carpenter, and L. M. Crowe. 1997. The role of vitrification in anhydrobiosis. *Annu. Rev. Physiol.* 60:73–103.
2. Hottiger, T., P. Schmutz, and A. Wiemken. 1987. Heat-induced accumulation and futile cycling of trehalose in *Saccharomyces cerevisiae*. *J. Bacteriol.* 169:5518–5522.
3. Hounsa, C. G., E. V. Brandt, J. Thevelein, S. Hohmann, and B. A. Prior. 1998. Role of trehalose in survival of *Saccharomyces cerevisiae* under osmotic stress. *Microbiology.* 144:671–680.
4. Wonisch, W., M. Hayn, R. J. Schaur, F. Tatzber, I. Kranner, D. Grill, R. Winkler, T. Bilinski, S. D. Kohlwein, and H. Esterbauer. 1997. Increased stress parameter synthesis in the yeast *Saccharomyces cerevisiae* after treatment with 4-hydroxy-2-nonenal. *FEBS Lett.* 405: 11–15.
5. Oliver, A. E., D. K. Hincha, and J. H. Crowe. 2002. Looking beyond sugars: the role of amphiphilic solutes in preventing adventitious reactions in anhydrobiotes at low water contents. *Comp. Biochem. Physiol. A Mol. Integr. Physiol.* 131:515–525.
6. Crowe, J. H., F. A. Hoekstra, and L. M. Crowe. 1992. Anhydrobiosis. *Annu. Rev. Physiol.* 54:579–599.
7. Hoekstra, F. A., E. A. Golovina, F. A. Tetteroo, and W. F. Wolkers. 2001. Induction of desiccation tolerance in plant somatic embryos: how exclusive is the protective role of sugars? *Cryobiology.* 43:140–150.
8. Wright, D. L., A. Eroglu, M. Toner, and T. L. Toth. 2004. Use of sugars in cryopreserving human oocytes. *Reprod. Biomed. Online.* 9: 179–186.
9. Doeven, K. D., J. H. A. Folgering, V. Krasnikov, E. R. Geertsma, G. van den Bogaart, and B. Poolman. 2005. Distribution, lateral mobility and function of membrane proteins incorporated into giant unilamellar vesicles. *Biophys. J.* 88:1134–1142.
10. Crowe, J. H., L. M. Crowe, A. E. Oliver, N. Tsvetkova, W. Wolkers, and F. Tablin. 2001. The trehalose myth revisited: introduction to a symposium on stabilization of cells in the dry state. *Cryobiology.* 43: 89–105.
11. Koster, K. L., Y. P. Lei, M. Anderson, S. Martin, and G. Bryant. 2000. Effects of vitrified sugars on phosphatidylcholine fluid-to-gel phase transitions. *Biophys. J.* 78:1932–1948.
12. Cacela, C., and D. K. Hincha. 2006. Low amounts of sucrose are sufficient to depress the phase transition temperature of dry phosphatidylcholine, but not for lyoprotection of liposomes. *Biophys. J.* 90: 2831–2842.
13. Roe, K., and T. P. Labuza. 2005. Glass-transition and crystallization of amorphous trehalose-sucrose mixtures. *Int. J. Food Prop.* 8:559–574.
14. Crowe, J. H., L. M. Crowe, J. F. Carpenter, A. S. Rudolph, C. Aurell Wistrom, B. J. Spargo, and T. J. Anchordoguy. 1988. Interactions of sugars with membranes. *Biochim. Biophys. Acta.* 947:367–384.
15. Crowe, L. M., R. Mouradian, J. H. Crowe, S. A. Jackson, and C. Womersly. 1984. Effects of carbohydrates on membrane stability at low water activities. *Biochim. Biophys. Acta.* 769:141–150.
16. Hincha, D. K., E. Zuther, E. M. Hellwege, and A. G. Heyer. 2002. Specific effects of fructo- and gluco-oligosaccharides in the preservation of liposomes during drying. *Glycobiology.* 12:103–110.
17. Luzardo, M., F. Amalfa, A. M. Nuñez, A. C. Biondi de López, and E. A. Disalvo. 2000. Effect of trehalose and sucrose on the hydration and dipole potential of lipid bilayers. *Biophys. J.* 78:2452–2458.
18. Crowe, L. M., and J. H. Crowe. 1991. Solution effects on the thermotropic phase transition of unilamellar liposomes. *Biochim. Biophys. Acta.* 1064:267–274.
19. Ohtake, S., C. Schebor, and J. J. de Pablo. 2006. Effects of trehalose on the phase behavior of DPPC-cholesterol unilamellar vesicles. *Biochim. Biophys. Acta.* 1758:65–73.
20. Elson, E. L., and D. Magde. 1974. Fluorescence correlation spectroscopy. I. Conceptual basis and theory. *Biopolymers.* 13:1–27.
21. Van der Spoel, D., E. Lindahl, B. Hess, A. R. van Buuren, E. Apol, P. J. Meulenhoff, D. P. Tieleman, A. L. T. M. Sijbers, K. A. Feenstra, R. van Drunen, and H. J. C. Berendsen. 2004. GROMACS user manual version 3.2. http://www.gromacs.org.
22. Oostenbrink, C., A. Villa, A. E. Mark, and W. F. van Gunsteren. 2004. A biomolecular force field based on the free enthalpy of hydration and solvation: the GROMOS force-field parameter sets 53A5 and 53A6. *J. Comput. Chem.* 25:1656–1676.
23. Berendsen, H. J. C., J. P. M. Postma, W. F. van Gunsteren, and J. Hermans. 1981. Interaction models for water in relation to protein hydration. *In* Intermolecular Forces. B. Pullman, editor. Reidel Publishing, Dordrecht, The Netherlands. 331–342.
24. Hockney, R. W. 1970. The potential calculation and some applications. *Meth. Comput. Phys.* 9:136–211.
25. Hess, B., H. Bekker, H. J. C. Berendsen, and J. G. E. M. Fraaije. 1997. LINCS: a linear constraint solver for molecular simulations. *J. Comput. Chem.* 18:1463–1472.
26. Miyamoto, S., and P. A. Kollman. 1992. SETTLE: an analytical version of the SHAKE and RATTLE algorithm for rigid water models. *J. Comput. Chem.* 13:952–962.
27. Berendsen, H. J. C., J. P. M. Postma, A. DiNola, and J. R. Haak. 1984. Molecular dynamics with coupling to an external bath. *J. Chem. Phys.* 81:3684–3690.
28. Tironi, I. G., R. Sperb, P. E. Smith, and W. F. van Gunsteren. 1995. A generalized reaction field method for molecular dynamics simulations. *J. Chem. Phys.* 102:5451–5459.
29. De Vries, A. H., A. E. Mark, and S. J. Marrink. 2004. The binary mixing behavior of phospholipids in a bilayer: a molecular dynamics study. *J. Phys. Chem. B.* 108:2454–2463.
30. Pereira, C. S., R. D. Lins, I. Chandrasekhar, L. C. G. Freitas, and P. H. Hünenberger. 2004. Interaction of the disaccharide trehalose with a phospholipid bilayer: a molecular dynamics study. *Biophys. J.* 86: 2273–2285.
31. Berman, H. M., J. Westbrook, Z. Feng, G. Gilliland, T. N. Bhat, H. Weissig, I. N. Shindyalov, and P. E. Bourne. 2000. The Protein Data Bank. *Nucleic Acids Res.* 28:235–242.
32. Schüttelkopf, A. W., and D. M. F. van Aalten. 2004. PRODRG—a tool for high-throughput crystallography of protein-ligand complexes. *Acta Crystallogr. D Biol. Crystallogr.* 60:1355–1363.
33. Lins, R. D., and P. H. Hünenberger. 2005. A new GROMOS parameter set for hexopyranose-based carbohydrates. *J. Comput. Chem.* 26: 1400–1412.
34. Marrink, S. J., A. H. de Vries, and A. E. Mark. 2004. Coarse grained model for semiquantitative lipid simulations. *J. Phys. Chem. B.* 108:750–760.
35. Kahya, N., D. Scherfeld, K. Bacia, B. Poolman, and P. Schwille. 2003. Probing lipid mobility of raft-exhibiting model membranes by fluorescence correlation spectroscopy. *J. Biol. Chem.* 278:28109–28115.
36. Fillipov, A., G. Orädd, and G. Lindblom. 2003. The effect on cholesterol on the lateral diffusion of phospholipids in oriented bilayers. *Biophys. J.* 84:3079–3086.
37. Saffman, P. G., and M. Delbrück. 1975. Brownian motion in biological membranes. *Proc. Natl. Acad. Sci. USA.* 72:3111–3113.

38. Skibinsky, A., R. M. Venable, and R. W. Pastor. 2005. A molecular dynamics study of the response of lipid bilayers and monolayers to trehalose. *Biophys. J.* 89:4111–4121.

39. Sum, A. K., R. Faller, and J. J. de Pablo. 2003. Molecular simulation study of phospholipid bilayers and insights of the interactions with disaccharides. *Biophys. J.* 85:2830–2844.

40. Wiener, M. C., and S. H. White. 1992. Structure of a fluid dioleoylphosphatidylcholine bilayer determined by joint refinement of x-ray and neutron diffraction data. II. Distribution and packing of terminal methyl groups. *Biophys. J.* 61:428–433.

41. Tristram-Nagle, S., H. I. Petrache, and J. F. Nagle. 1998. Structure and interactions of fully hydrated dioleoylphosphatidylcholine bilayers. *Biophys. J.* 75:917–925.

42. Kučerka, N., S. Tristam-Nagle, and J. F. Nagle. 2005. Structure of fully hydrated fluid phase lipid bilayers with monounsaturated chains. *J. Membr. Biol.* 208:1–10.

43. Chandrasekhar, I., D. Bakowies, A. Glättli, P. H. Hünenberger, C. Pereira, and W. F. van Gunsteren. 2005. Molecular dynamics simulation of lipid bilayers with GROMOS96: application of surface tension. *Mol. Simul.* 31:543–548.

44. Marrink, S. J., E. Lindahl, O. Edholm, and A. Mark. 2001. Simulation of the spontaneous aggregation of phospholipids into bilayers. *J. Am. Chem. Soc.* 123:8638–8639.

45. Gambin, Y., R. Lopez-Esparza, M. Reffay, E. Sierecki, N. S. Gov, M. Genest, R. S. Hodges, and W. Urbach. 2006. Lateral mobility of proteins in liquid membranes revisited. *Proc. Natl. Acad. Sci. USA.* 103:2098–2102.

46. Nagase, H., H. Ueda, and M. Nakagaki. 1997. Effect of water on lamellar structure of DPPC/sugar systems. *Biochim. Biophys. Acta.* 1328: 197–206.

47. Vaz, W. L., J. Stümpel, D. Hallmann, A. Gambacorta, and M. de Rosa. 1987. Bounding fluid viscosity and translational diffusion in a fluid lipid bilayer. *Eur. Biophys. J.* 15:111–115.

48. Ollmann, M., A. Robitzki, G. Schwarzmann, and H. J. Galla. 1988. Minor effects of bulk viscosity on lipid translational diffusion measured by the excimer formation technique. *Eur. Biophys. J.* 16:109–112.